Fenton-Enhanced zero-valent iron powder oxidation: Investigating transformation products of antimicrobials and its removal

Anuradha Goswami[1,2*], Jia-Qian Jiang[1**], Roberts Joanne[1], Michael Petri[3]

[1] School of Engineering and Built Environment, Glasgow Caledonian University, Glasgow G4 0BA, Scotland, United Kingdom; [2] Department of Biology, The University of Alabama at Birmingham, Birmingham, Alabama USA; [3] Zweckverband Bodensee-Wasserversorgung, Süßenmühle 1, 78354 Sipplingen, Germany

*Corresponding: anugos24@uab.edu; ** Co-corresponding: jiaqian.jiang@gcu.ac.uk

Abstract

The occurrence of pharmaceuticals and pesticides in water is of concern due to their hazardous effect on the environment. Such micropollutants deteriorate environmental quality and can induce antimicrobial resistance in pathogenic bacteria. Thus, removal of these emerging contaminants is a necessity and thus requires a clear understanding of the effective treatment and mechanistic approach utilized in degradation and removal. Frequently, treatment systems are optimized for the removal of contaminants while the formation of transformation products and their removal are not targeted. We utilized our established iron powder catalyzed Fe (0) Fenton Oxidation treatment to study the degradation of emerging contaminants — sulfamethoxazole, gabapentin, diuron, and triazine class pesticides. We used state-of-the-art mass spectrometry to establish the common oxidative mechanistic approach after identifying the transformation products formed during the Fe (0) Fenton Oxidation processes. Fenton transformed product was produced after 60 min reaction time when treatment was initiated after adding the optimized H_2O_2 and iron powder Fe (0)) in a micropollutant solution adjusted to pH 5. About 5-to-7 transformed products of each micropollutant were identified and predicted to have low toxicity risk to aquatic organisms. The oxidative degradation pathway of micropollutants illustrates the shared oxidative mechanism where the aliphatic chain of the heteroatom: Sulphur (R—S—R as thiosulphate), functional groups (R—C=O, R—COOR, R—NH$_2$, R—NH=O—N) and alkyl chain present in the target compound was suggested as the prime region of hydroxyl radicle (•OH) attack. The tandem mass spectrometry estimated the evolution of sulfamethoxazole-transformed product formation and removal during the treatment. The informed optimization of Fe (0) Fenton treatment, confirmed through MS^2 was established at 40 min reaction time at which both the sulfamethoxazole and its transformed product were reduced to trace levels (ngL^{-1}).

Introduction

Antimicrobials are organic compounds that effectively kill or stop the growth of microbes. These can include antibiotics, pharmaceutical residues, or pesticides/herbicides[1]. The widespread detection of antimicrobial compounds in surface and groundwater has become a profound global concern with multifaceted consequences[2]. The presence of antimicrobials in water contributes to the development of antimicrobial resistance (AMR)

40 which is an increasing problem for the environment and human health[3]. In 2019, the World
41 Health Organization (WHO) identified AMR as one of the top ten threats to world health and
42 advocated for reducing AMR transmission from all probable sources[4]. In recent years,
43 efforts to remove antimicrobials and other contaminants of emerging concerns involve
44 several physical, biological, and chemical methods. The rationale behind using physical
45 methods such as filtration and sedimentation is removing pollutants from water by
46 transferring them to another phase but does not degrade the compound. Biological methods
47 such as activated sludge treatment and biological membrane degradation are widely used
48 to degrade organic contaminants. Despite the efficacy of biological treatment in removing
49 certain micropollutants, challenges persist in achieving complete degradation of a diverse
50 array of these contaminants. Moreover, conventional biological processes often generate
51 substantial sludge volumes, contribute to greenhouse gas emissions, and necessitate high
52 energy inputs [5]. These limitations underscore the need for complementary or alternative
53 treatment technologies.

54 Disinfection and solid-liquid separation methods are proven to efficiently remove dissolved
55 and colloidal solids rather than optimized to transform antimicrobials into non-toxic
56 compounds. Moreover, most water treatments estimate the degradation of the parent
57 compound, but identifying transformed by-products during the treatment is profoundly
58 overlooked. The by-products formed as residuals from incomplete mineralization of
59 micropollutants removal in water treatment, which may exhibit similar or relatively greater
60 toxicity to the parent compound is a prime concern in water reclamation facilities. In our
61 previous study, we identified that substituting iron salt in a conventional Fenton process
62 with micron-sized iron powder overcame the sludge production challenge and resulted in
63 non-toxic oxidized pharmaceuticals and pesticide (antimicrobials) residues. The synergistic
64 action of iron powder [Fe (0)] – oxidative and adsorptive in a heterogenous Fenton process
65 exhibits about 70% mineralization rate of micropollutants[6]. The interconversion of iron
66 species to Fe^{2+} and Fe^{3+} functioned as a catalyst and facilitated the Fenton reaction,
67 nevertheless, the degradation by-products were also absorbed onto the microporous Fe (0)
68 surface. This conjunction of dual action mechanisms reduced effluent toxicity, signifying a
69 promising emerging technology in Fenton treatment [6, 7].

70 We developed a heterogeneous Fenton Fe (0) that was more favorable to micropollutant
71 removal compared to homogeneous Fenton (Fe^{2+}) due to the oxidative effect of •OH in
72 solution and the spatial adsorption of by-products on the Fe catalyst [7]. A study by Trellu et
73 al., 2018 [8], demonstrated that •OH oxidizes phenol adsorbed onto activated carbon cathode
74 in an electro-Fenton treatment, thus enhancing the micropollutant mineralization. Similarly,
75 we suggested putative pathways for micropollutant mineralization through Fe(0), which
76 specifies the production of degenerative by-products via four possible pathways namely*, i)*
77 adsorption of the compound on Fe(0), ***ii)*** oxidation of micropollutant, ***iii)*** adsorption of the
78 oxidized compound on Fe(0) and ***iv)*** oxidation of oxidized by-products [6]. Overall, Fenton
79 Chemistry plays a significant role in environmental applications, particularly in the
80 treatment of contaminants. Principally, the Fenton reaction occurs naturally in several
81 environmental settings. Surface water when exposed to sunlight can generate hydrogen

82 peroxide through photochemical reactions. Hydrogen peroxide can degenerate to hydroxyl
83 radicals in the presence of iron and can initiate the Fenton reaction[9]. The occurrence of these
84 reactions in a natural environment is evident from the presence of superoxide dismutase
85 enzyme in microbes which protects against oxidative stress[10]. Therefore, identifying the
86 oxidation by-products of compounds with potency to impact environmental and human
87 health is critical.

88 The current study is the extended assessment of Fe (0) Fenton Oxidation, and we have
89 proposed the degradation pathways of common antimicrobials namely, sulfamethoxazole,
90 gabapentin, and pesticides- diuron and triazine (terbutryn, terbuthylazine) to non-toxic
91 oxidized transformation products in Fe (0) Fenton Oxidation Process. The acute toxicity of
92 diuron and antimicrobial properties of studied compounds was previously studied[11]. The
93 formation of an oxidized transformed product (TPs) of each analyte after Fenton treatment
94 was evaluated to predict the degradation pathway. The sulfamethoxazole was further
95 investigated to detect and quantify the formation of oxidized TPs as a function of time during
96 the Fe (0) Fenton Oxidation Process. The results of this study provide insightful information
97 on the degradation of selected pharmaceuticals and pesticides. Identifying the temporal
98 evolution of sulfamethoxazole broadens the avenue of scientific inquiry to understand the
99 formation and fate of sulfa-drug and develop a water treatment focusing on identifying and
100 removal of toxic parent and transformed products.

101 **Compound selection criteria and its properties**

102 **1. Sulfamethoxazole**

103 Sulfamethoxazole [4-amino-N-(5-methyl-1,2-oxazol-3yl) benzene sulfonamide], is used as
104 an antibiotic against bacterial infections. These drugs are commercially available as 500 mg
105 and 1 g capsules and 500 mg $(5ml)^{-1}$ oral solution. The primary therapeutic use of this drug
106 has been in the curing of acute urinary tract infections, respiratory tract infections
107 (Pneumocystis carinii), meningitis, gonorrhea, and several systemic infections[12]. The
108 chemical structure and its physicochemical details are presented in Table 1.
109 Sulfamethoxazole is sparingly soluble in water, however low K_{OC} value is conducive to
110 leaching potential. The International Agency for Research on Cancer monographs volume
111 79 (IARC) evaluates sulfamethoxazole as a carcinogenic potency after prolonged
112 prescription to animals and humans. Sulfamethoxazole residuals in water pose a threat to
113 human health, and the ecosystem, therefore, requires scientific outreach for the
114 identification of transformed products and removal techniques.

115 **2. Gabapentin**

116 Gabapentin [1-(Aminomethyl) cyclohexyl) acetic acid] is used with other medications to
117 prevent and control seizures[13]. These are available in 100 to 400 mg capsules and oral
118 $250mg-5mL^{-1}$ solution[14]. Gabapentin's chemical structure and its physicochemical
119 properties are given in Table 1, respectively. Gabapentin is commonly found as unchanged

120 drug residues in the environment due to minimal metabolism in the human body[15]. The
121 presence of gabapentin in the environment raises concerns about its environmental
122 impacts and may contribute to changes in microbial ecology, particularly selecting for
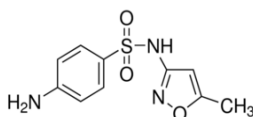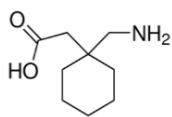123 antimicrobial resistance[16].

3. Diuron

125 Diuron [3-(3,4-dichlorophenyl)-1,1-dimethylurea], largely used as pre- and post-emergent
126 herbicide treatment on varieties of crops, an algaecide in commercial fish production[17].
127 Diuron is also applied as pre-emergence control of annual broadly leafed grass and
128 perennial weeds[18]. A report from the Environmental Fate and Effects Division, Washington,
129 D.C. concluded that diuron contamination in groundwater in California was detected in the
130 2-to-3 ppb range, whereas the elevated levels pose a hazard to aquatic life and can have
131 human health implications[19]. The chemical structure of diuron and its physicochemical
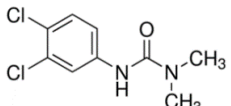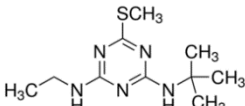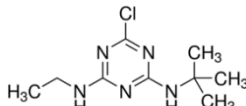132 properties are given in Table 1, respectively.

4. Triazines (Terbutryn and Terbuthylazine)

134 Terbutryn and terbuthylazine are selective herbicides that belong to the Triazines class.
135 Triazines are absorbed by the roots and foliage and act as an inhibitor of photosynthesis.
136 These compounds are toxic and tend to accumulate in the environment causing prolonged
137 pollution[20 20, 21]. The molecular structure and physicochemical properties of triazines are
138 described in Table 1.

139 **Table 1** Physio-chemical properties of micropollutants of interest studied in this research

Pharmaceuticals		
Compound	**Sulfamethoxazole**	**Gabapentin**
Class	Antibiotic	Anticonvulsant
Acid dissociation constant (pKa)	6.1	3.68 (Carboxylic acid); 10.70 (primary amine) at 25 ºC
Structure		
Potential hazard	Carcinogen, hazardous to aquatic environment mutagen promotes antimicrobial resistance	Carcinogen, hazardous to aquatic, skin sensitizer, suggested antimicrobial activity
Herbicide/ Pesticide		
Compound	**Diuron**	**Terbutryn** **Terbuthylazine**

Class	Dimethyl urea	Triazine	Dimethyl urea
Acid dissociation constant (pKa)	13.55 (weak acid)	4.3	1.95 at 20 °C
Structure			
Potential hazard	Carcinogen, hazardous to aquatic ecosystem, suggested antimicrobial activity	Carcinogen, hazardous to aquatic ecosystems, acutely toxic via the oral route, suggested antimicrobial activity	Carcinogen, hazardous to aquatic ecosystem, acutely toxic via the oral route, suggested antimicrobial activity

Experimental

Chemicals

All micropollutants used in this study were purchased from Sigma Aldrich. 2.5LT Methanol, for HPLC, was purchased from Fischer Scientific and was used in LC-MS/MS gradient. Fe powder(fine) [Item Code 12310] used as a catalyst in the Fenton experiment was purchased from Sigma Aldrich. Hydrogen peroxide, for analysis, 35 wt.% solutions in water, stabilized, ACROS Organics™ used as an oxidant in the Fenton experiment was purchased from Fischer Scientific. Sodium hydroxide and Sulfuric Acid Min 95% d=1.83, Certified AR used to adjust pH was purchased from Fisher Scientific. The Kemira flocculator 2000 was used to conduct the Fenton Oxidation water treatment experiments.

Experimental Setup

a) Fe (0) – Fenton Oxidation Process batch experiment

The calibrated DENVER INSTRUMENT weighing balance was used throughout the research to weigh solid chemicals. The working solution of 0.1 and 5 mg L^{-1} was prepared from freshly prepared 1 and 10 mg L^{-1} stock solutions in distilled Milli Q water, respectively. The pH of the micropollutants spiked solution was adjusted to pH 5 after adding iron powder using 1 N NaOH and 1N H_2SO_4 and measured using an EUTECH CyberScan pH 11 pH/mV/°C meter coupled with EUTECH Instruments electrodes. Each experiment was conducted in a batch process system and the effluents were collected after the treatment. Fenton experiments were conducted at ambient room temperature, 20±5°C, and atmospheric pressure in one-liter glass beakers. The 1L volume solution was mixed with horizontal stirring vanes at 400 rpm for one minute and 80 rpm for adequate reaction time. The optimized experimental conditions of selected micropollutants used to estimate the micropollutant degradation at

pH 5 are listed in Table 2. The transformation products were studied at the same experimental condition where 5 mg L^{-1} of the initial solution adjusted to pH 5 was run for 60 60-minute reaction time for every micropollutant. The system remained undisturbed for 30 min after the treatment to deploy the sedimentation process.

The effluent was collected after sedimentation and vacuum filtration. The iron particles from the iron powder adhered to the walls of the container and were removed after filtration. The 100 ml sample was filtered through 0.45 μm filter paper (MFTM membrane filters, nitrocellulose membranes, Merck Millipore Ltd.) The filtered samples were stored in 100 ml storage glass bottles at ~2-4°C (purchased from Fischer Scientific UK) for up to three days and used in the analysis.

Table 2 Fe (0) Fenton Oxidation Process optimization conditions for sulfamethoxazole, gabapentin, diuron, terbutryn, and terbuthylazine

Micropollutant	Reaction time (min)	H_2O_2: Fe (0)
Sulfamethoxazole	60	0.9:1
Gabapentin	45	0.9:1
Diuron	45	3.5:1
Terbutryn	15	3.5:1
Terbuthylazine	15	1.3:1

b) Transformation products identification in Fe (0) Fenton Oxidation

The 5 mg L^{-1} of each analyte solution was prepared in fresh Milli Q water from a serial dilution of freshly prepared 10 mg L^{-1} standard solution. The experiment was conducted with the same moles of Fe (0) and H_2O_2 optimized earlier for 1mg L^{-1} but using a higher concentration of the analyte to detect observable peaks [6, 7]. The pH of the analyte was adjusted to five using 0.1M NaOH and Fe (0) Fenton treatment was run for 60 min before effluent collection. In addition, sulfamethoxazole was also subject to complete oxidation for product-ion fragmentation and by-product evolution as a function of time during the treatment. As a control experiment, Milli Q water was processed through the same Fenton oxidation experimental condition, and the full MS scan of the control was subtracted from the obtained peak. Before analysis, the treatment effluent was filtered through Fisherbrand™ Non-sterile Nylon Syringe Filter, 25 mm diameter, 0.2 μm filters. The filtrate (one mL) was collected in Thermo Scientific™ 9mm Clear Glass Screw-Thread Vials, stored at 4°C, and analyzed within three to four days.

Instrumentation and LC-MS operating conditions LC-MS Master method development for identification of unknown compounds

The LC-MS master method consists of an acquisition and processing method. An acquisition method is the multiple-step instruction fed into the LC-MS to identify unknown organic compounds formed during the Fe (0) Fenton treatment. It includes the Liquid chromatography (LC) and High-resolution Mass spectrometry (HRMS) methods. The LC

195 method includes the column used, mobile phase, injection volume, flow rate, and run time
196 as given in Table 3. The analyte was first fully scanned from the 50 to 750 mass range to
197 obtain its retention time. The gradient method was incorporated to separate the individual
198 analytes at specific retention times effectively. The gradient information of the mobile phase
199 on percentage contribution depending on retention time was developed. The solvents A
200 (eluent A) and B (eluent B) were the organic and aqueous mobile phase.

201 The liquid elution gradient begins with 99% of the total volume of eluent A (0.1% Formic Acid
202 in Milli Q water) in the aqueous phase while 1% eluent B (0.1% Formic Acid in methanol) in
203 organic solvent was held for an initial one minute. At the second minute, eluent A dropped
204 down to 60%, and eluent B rose to 40% and was held up to four minutes. Then, eluent A was
205 again raised to 99%, and eluent B dropped to 1%. The eluent was held until seven minutes
206 and then, reversed (eluent A: 1%, eluent B: 99%) and maintained along the run time. The data
207 processing including peak adjustment, generating calibration curve, and quantification was
208 performed in Thermo Fischer Scientific TraceFinder™ software. Detailed information on the
209 LCMS instrumentation and method is provided in the Supplemental file S1. The calibration
210 curve was constructed using linear regression with a $1/x^2$ weighting factor to achieve the
211 curve stability and quantification data quality. A deviation higher than +/- 20% from the best-
212 fit curve was not considered while plotting the calibration lines. From the deviation (%
213 difference), the quantification limit of micropollutants was examined. The calibration curves
214 of each compound were prepared from 10000 ng mL^{-1} to 1 ng mL^{-1} range. The lower limit of
215 quantification established from calibration standards was – Sulfamethoxazole and Diuron
216 (25 ng mL^{-1}), Gabapentin, Terbutryn, and Terbuthylazine (1 ng mL^{-1}).

217 **Table 3** LC-MS method used to detect the micropollutants of interest in this study

LC Column	Waters™ Xselect HSS column XP
	diameter 2.1 x 150 mm, particle size 2.5 µm
Mobile Phase	Eluent A: 0.1 % Formic Acid in Milli Q water
	Eluent B: 0.1 % Formic Acid in Methanol
Injection Volume	250 µl
Flow rate	3 µl min^{-1}
Run time	0 to 17 min

218 The samples to be analyzed were placed in a chilled (~ 10°C) sampler unit. The adequate
219 volumes of samples as designed in the method were injected into the column where the
220 analytes were separated and later entered the ion source. The ion source ionized the
221 compound and analyzed based on its mass-to-charge ratio (m/z). The Dionex Ultimate 3000
222 RS pump was used to move samples through the LC column, separating components of a
223 mixture based on their interactions with a stationary phase. The nitrogen gas sprayed at a
224 voltage of 3500 V, in the Orbitrap Electrospray Ionization (ESI) converts the eluted
225 components into ions for mass analysis, detected at 17,500 ppm resolution. The
226 Quadrupole mass filter was used to filter selected ions, and C-Trap was used for short pulse

227   injection and ion accumulation of selected ions as temporary storage. The precursor ions
228   were purged through the Collision cell for High Energy Collisional dissociation to generate
229   product ions and the Orbitrap analyzer installed was used to perform the Fourier transform
230   mass analysis.

Identification of oxidation by-products in LC-MS/MS

232   The targeted analysis was used to identify the oxidation by-products. The database of
233   precursor ion mass was curated from previous literature studying the oxidation by-products
234   of the analyte of interest[22][23][24]. As of date, and Web of Science search we couldn't find
235   literature studying oxidation by-products using Fe (0): iron powder Fenton Oxidation and thus
236   we were restricted to literature mainly focused on ozonized and photocatalytic oxidation
237   treatment. The inclusion list of analytes was derived after m/z analysis of each compound
238   for the obtained retention time in HRMS. The full MS scan (50 –to– 750 m/z) identifies the
239   compounds on the mass-to-charge ratio (m/z) to derive the retention time and precursor ion
240   information. The mass error was estimated from the accurate experimental mass checked
241   against the exact calculated mass using the mass accuracy equation. The exact calculated
242   mass was obtained from the in-house curated database constructed from ChemCal
243   database search and published literature, discussed later in results. The mass accuracy
244   (mass error) of ±5 ppm for precursor ions and ±10 ppm for product ions was considered
245   significant and are discussed in this study.

246
$$\textbf{Mass accuracy} = (\frac{Accurate\ experimental\ mass - Exact\ calculated\ mass}{Exact\ calculated\ mass}) \times 10^6$$

247   The retention time and precursor ion data of each analyte were fed into the MS acquisition
248   method to obtain the product ions information. The fragmentation patterns of product ions
249   served as a fingerprint and were used to accurately identify the precursor ions and their
250   oxidized by-product compounds. The m/z of precursor ion and their product ions fed into the
251   inclusion list are mentioned in Supplemental file S1. The retention time and chromatogram
252   peaks of each analyte precursor and product ion are provided in Supplemental Figure 1.
253   Different isomers with the same precursor ion were differentiated after product ion
254   scanning. The neutral loss- the loss of a neutral molecule from the precursor ion during the
255   fragmentation in MS/MS was estimated by calculating the difference between m/z of the
256   product ions from the precursor ion. The characteristics of neutral losses in product ion
257   spectra were used to identify the functional groups.

258   Diuron and gabapentin oxidation by-products were identified in both ESI (+) and ESI (-). The
259   remaining compounds were only detected in ESI (+). The high resolution of MS yields
260   accurate mass measurements and permits structural elucidation. The accurate
261   experimental mass obtained was fed into the ChemCal web interface database[25] to predict
262   the molecular formula. The molecular formulae were confirmed after the isotope analysis.

263   The structures predicted in this study were also referred to previous literature for
264   confirmation. However, the obtained m/z was only validated after mass accuracy
265   calculation. The chemical structure was assigned with regard to the parent compound and
266   based on the chemistry of Fenton Oxidation reactions. The structure and their nomenclature
267   illustrated in Supplemental S4 were generated from the ChemSketch application software
268   and RCSB PDB Chemical Sketch Tool available online at https://www.rcsb.org/chemical-
269   sketch [26]. The mass spectral data was further studied to identify the structure configuration
270   and provide confirmation after matching up the isotope pattern of the compounds.

Parallel reaction monitoring (PRM): Sulfamethoxazole fragment pattern quantification

272   The retention time and precursor ion data of oxidized by-products of sulfamethoxazole were
273   fed into the MS acquisition method to obtain the product ions information. The fixed
274   precursor ions scan – single experiment to determine the m/z of product ions produced by
275   the reaction of a selected precursor ion with sulfamethoxazole and its by-product precursor
276   ion m/z at tandem mass spectrometry (MS/MS) at 35 collision energy resolution. The PRM
277   software was fed with the precursor ion information added as an inclusion list. The inclusion
278   list was used by software to estimate the product ions of the by-products. The isolation
279   window of 2 was set for estimation validation. The isolation window in PRM is similar to the
280   Mass Accuracy in Full MS scans mentioned before. After feeding precursor ion information
281   in the acquisition method, the '*Estimate*' standard type was selected and linked to the parent
282   analyte (sulfamethoxazole). An approximate estimation of by-product concentration was
283   made from surrogate parent analytes calibration. This step provided strong evidence of the
284   structural configuration. The change in sulfamethoxazole by-product concentration as a
285   function of time in the Fe (0) catalytic Fenton oxidation treatment was estimated from the
286   surrogate calibration curve of sulfamethoxazole

Rate of change in sulfamethoxazole and its transformed products

288   The rate of sulfamethoxazole and its TPs formation and oxidation at consecutive time
289   intervals was estimated using the established optimized Fe (0)-Fenton Process. A previously
290   optimized dose of 23.31 mM H_2O_2 and 27.25 mM iron powder [Fe (0)] was added to the 1 mg
291   L^{-1} sulfamethoxazole solution prepared in Milli Q water. The pH of the initial solution was
292   adjusted to five before initiating the reaction. The rate of change (Δ) in sulfamethoxazole and
293   the formation or disappearance of its transformed products as a function of time during the
294   Fe (0)- Fenton Process was estimated as a ratio of the difference in m/z intensity of ions at a
295   given time (t) from its initial intensity and difference in treatment time (t- 1), given below.

296
$$\text{Rate of Change in compound} = \frac{\Delta m/z}{\Delta t}$$

change in mass intensity $\Delta m/z$ between consecutive time points = [m/z^{time} — $m/i^{initial}$]; m/t^{ime} is m/z intensity of ions at time point t (min) and m/i^{initial} is m/z intensity of ions at time point t = 1 min.

Ecological Structure Activity Relationship (ECOSAR) to predict toxicity of transformed products

The ECOSAR Program tool v.2.2 developed by the US EPA was used to predict the toxicity of transformed products using the quantitative structure-activity relationships (QSAR) model. It groups structurally similar chemicals with available experimental effect levels in aquatic organisms – Fish, Daphnids, and Green algae. The SMILES (molecular text code) consists of the chemical structure of the parent compound and transformed products generated from the RCSB PDB [26] were fed into the software to predict the acute toxicity measured by the half minimal effective concentration (EC_{50}), lethal concentration (LC_{50}) and chronic toxicity of the tested compound.

Results

Zero-valent iron (Fe (0)) catalyzed Fenton oxidation demonstrated high efficacy in the degradation of target micropollutants at pH 5

We examined the degradation efficiency of a suite of emerging micropollutants hazardous to aquatic ecosystems with accredited antimicrobial activity. In our previous study, we have established the synergistic contribution of zerovalent iron powder catalyzed Fenton Oxidation via oxidation and sorption mechanism, yielding non-toxic effluent water quality [6]. At optimal pH 3 treatment conditions, the Fe (0) Fenton achieved complete degradation and about 70% mineralization of selected micropollutant [7][6]. Herein, we tested the degradation efficiency of target micropollutants at pH 5 after initiating the Fenton reaction using a similar H_2O_2: Fe (0) optimized dose developed in our previous study [6]. The heterogeneous Fenton achieved from Fe (0) iron powder at pH 5 led to significant degradation efficiency for sulfamethoxazole, gabapentin, diuron, terbutryn, and terbuthylazine. Notably, terbutryn and sulfamethoxazole (98.42±2.74%) were among the highly degraded micropollutants followed by diuron (94.69±4.52%), gabapentin (85.91±6.14%) and terbuthylazine (69.21±2.07%), refer Figure 1. While overall degradation was promising, significant differences (p-value < 0.05) among diuron and terbuthylazine, terbutryn, and terbuthylazine were observed. These differences in the spontaneity of Fenton treatment might be attributed to structural variations among the compounds.

Studying the transformation products of varied molecular structures makes it crucial to understand the degradation pathway of zero-valent iron powder (Fe (0)) Fenton Oxidation. The low-intensity LC/MS peaks were obtained at treatment optimal conditions, and therefore, we opted for a higher micropollutant concentration (5mgL^{-1}) to detect the transformed oxidized products in the Fe (0)-Fenton Process. The compromised oxidation

condition attributed to micropollutant degradation in Fe (0) Fenton Oxidation was reasonable to observe oxidation products for the given treatment conditions. In addition, the sulfamethoxazole was also analyzed at optimum H_2O_2 and Fe (0) dose (implying complete oxidation), to produce a descriptive analysis of sulfamethoxazole reduction reciprocating to an increase in by-products formation with the development of treatment as a function of reaction time. The experimental conditions used to detect transformed products are described in the method section.

Structural elucidation of transformed products in iron powder (Fe (0)) facilitated — heterogeneous Fenton Oxidation Process

Based on the polarity and functional group of the parent compounds (micropollutants) the ionization mode to identify the transformed product was chosen. The initial and final solution after the Fe (0) Fenton experiment was scanned through a full MS scan m/z (50-to-750). The Milli Q water subjected to the Fe (0) Fenton experiment without spiking micropollutants was used as a blank (control) to subtract the control mass spectrum peak from the test solution obtained peak. The retention time and ion chromatogram of parent compounds and their TPs are given in Supplemental S2 and S3. Briefly, diuron and gabapentin TPs studied in both ESI (+) and ESI (-) identified – *i)* three positive ionization and four products in negative ionization of diuron TP's; *ii)* four and one gabapentin oxidation products in positive and negative ionization, respectively. Sulfamethoxazole, terbutryn, and terbuthylazine TPs were studied in ESI (+) and identified six, six, and five TP's, respectively.

The distribution of TP's and its isotopes are illustrated in Figure 3 and summarized in Supplemental S4. The mass accuracy of abundant TP's precursor ion and the relatively less prevalent isotopes were used for the structural confirmation. We identified 29 significant TPs in total, after Fe (0) Fenton Oxidation treatment of each micropollutant. The mass errors between ±5ppm of the transformed products and its isotopes between ±10ppm were proposed here after meeting the m/z ratio significant standards. By comparing the accurate experimental and exact calculated m/z ratio, the molecular formula of TPs was predicted. The observed isotope pattern further confirmed the elemental composition and structural configuration was then confirmed from previously published literature and observed the same TPs after oxidation of respective micropollutants [22] [23] [24] [27] [28].

To note, a sulfamethoxazole transformed product TP6-254 has an m/z ratio similar to the sulfamethoxazole but, was eluted at different retention times. The product was referred to sulfamethoxazole calibration peaks and analyzed for impurity. The compound was not found in standards and hence was confirmed as an oxidized transformed product. The retention time and mass spectrum of sulfamethoxazole, TP6-254, and similar product ions presented in Supplemental S5 identify TP6 m/z 254 eluted at 5.04 and 5.8 min while sulfamethoxazole retention time peak was obtained at 4.51 min. Thus, we concluded that the TP6-254 was either formed after the re-arrangement of sulfamethoxazole molecules or an N-oxide formation after oxidation of primary amine attached to the aniline ring structure.

373 A similar product was also observed in a study shown in[29, 30 22], and the plausible structure
374 configuration of TP6-254 was drawn using the same reference.

Transformation of sulfamethoxazole product as a function of time in Fe (0)- Fenton Oxidation Process

377 The elemental composition of sulfamethoxazole TPs was further examined from the
378 fragment ion pattern in tandem mass spectrometry (MS/MS) experiments. The ions of the
379 TPs of sulfamethoxazole detected in the mass analyzer were subjected to High Energy
380 Collisional Dissociation (HECD) after collision with nitrogen gas atoms in the collision cell
381 produced a specific fragment pattern of its product ions. These product ions were exclusive
382 and were also called the fingerprints of respective precursor ions. The product ion m/z 156
383 was detected for TP6-254 parent compound sulfamethoxazole (Supplemental S5) and thus
384 was continued for the elemental composition analysis. Similarly, the product-ion peaks of
385 TP3-284 were very insignificant thus no detectable fragment pattern was observed.

386 The fingerprints of TP1-270, TP2-272, TP4-288, and TP5-99 are presented in Figure 4 (a-d).
387 The precursor ion TP1-270 was fragmented at the sulfonamide bond to produce a product
388 ion m/z 172, after the loss of a neutral fragment$C_4H_6N_2O$ (m/z 94). Similarly, TP5-99
389 undergoes fragmentation resulting in the loss of a neutral fragment CHN (m/z 99) and results
390 in a product ion with m/z 72. The TP2-272 fragmented into several ions where the key
391 fragment ions and their potential origins (neutral loss NL) include m/z 156 (NL 116.0593),
392 m/z 140 (NL 132.0541), m/z 117 (NL 155.0046), m/z 108 (NL 164.0261), m/z 92 (NL 180.0210)
393 and m/z 73 (NL 199.0307). The TP4-288 key fragment patterns include m/z 156.0123: Loss of
394 a neutral fragment with a mass of 132.0542. m/z 174 (NL 114.0432), m/z 133 (NL 155.0045),
395 m/z 115 (NL 173.0153), m/z 108 (NL 180.0211) and m/z 92 (NL 196.0160). The proposed
396 structure of each transformed product predicted after the literature survey was further
397 confirmed by the fragmentation pattern. Overall, the presence of hydroxyl (OH) groups and
398 a nitrogen atom in the proposed structure suggests potential fragmentation sites involving
399 these functional groups. The loss of neutral fragments containing oxygen and nitrogen atoms
400 was also evident in most of the fragmentation patterns observed for the sulfamethoxazole
401 TPs.

Rate of occurrence and removal of sulfamethoxazole transformed in Fe (0)- Fenton Oxidation process.

404 The evolution of TPs, illustrated in Figure 4(e) reflects the insights of sulfamethoxazole
405 degradation and formation or removal of several TPs as a function of time. Incorporating the
406 information on TP evolution can further optimize the experiment after the selection of the
407 best reaction time for the complete removal of the parent compound and targeted TPs. The
408 relative strength of the TPs was estimated using a surrogate sulfamethoxazole standards
409 calibration curve. However, the estimated level was below the detection limit (1ng mL^{-1}) and
410 thus plotted against their peak area. The peak area obtained in LC/MS was used to estimate

the relative concentration. The sulfamethoxazole was completely degraded after 40 min of reaction while in-between oxidation reactions led to the formation of TPs. As indicated by the low m/z area of TP3-284, we found that relative to the rest of the TPs, TP3-284 was formed at the beginning of the treatment and was removed after 10 min.

In contrast, TP4-288, a compound with a parent ion peak at m/z 288.0665, was initially detected at trace levels during the early stages of the Fe (0)-Fenton oxidation process. Its signal remained below the limit of detection for approximately 35-to-40 minutes. Subsequently, a rapid increase in TP4-288 abundance was observed, culminating in a maximal signal intensity at the 60-minute mark of the reaction. Similarly, TP2-272 abundance was increased at the later stages of the treatment, that is between 45 to 60 min. TP1-270 demonstrated a definite pattern where its abundance was rapidly increased until the first 30 min of reaction – indicating hydroxylation after the addition of the OH group to sulfamethoxazole, but m/z intensity was detected at a trace level after 30 min. Refer to Supplemental S6 to find the exact m/z intensity of each studied at different time intervals of the treatment. Overall, the rate of degradation of sulfamethoxazole and its TPs at tested H_2O_2 and Fe (0) dose and initial solution pH 5, suggests 40 min as the optimum reaction time for the Fe (0)-Fenton Oxidation process of sulfamethoxazole.

Proposed degradation pathway for the Fe (0) Fenton Oxidation of antimicrobials

The degradation pathway of each studied compound presented in Figure 5 (a-e) was predicted after concluding the structure of TPs from the product and literature survey. The aromaticity, electronegativity, presence of functional groups, and polarizability determine the susceptibility to different types of reactions during the oxidation of analyte in the Fenton experiment. At pH 5, sulfamethoxazole (4-amino + H+) and terbuthylazine (3-N + H+) remove H+ from the solution whilst gabapentin loses its H+ ions (-COOH – H+). The sulfamethoxazole has an olefinic double bond and an aniline group which has a high affinity for OH radical attack [22]. The very prominent reaction pathway of OH radical was observed in the double bond located on the isoxazole ring. The OH radicals bind to C=C by H-abstraction or an electron transfer forming TP1-270 and TP2-272 respectively. The addition of OH to the C=C bond (TP1-270) led to the formation of a tertiary carbon atom-centered radical-mediated another C-OH bond (TP4-288). The oxidation of the tertiary amino group (in aniline structure) could form a tertiary-NO_2 compound (TP3-284). The amino group triggered by the radical attack would have facilitated the electrophilic substitution nitration process. Next, TP5-99 was predicted to be formed from the hydrolytic cleavage of the sulfamethoxazole cleavage. The same mass was also detected in fragment pattern analysis and therefore, could have also been arising from the further breakdown of the transformed products.

The gabapentin oxidized products were found to be more polar than the parent compound in this study and previously by Hermann et al.,2015 [27]. The gabapentin degradation pathway shown below in Figure 5 (b) demonstrates the strong oxidative effect of the OH radical. TP1-188 was formed after the radical attack causing the elimination of the H-atom from the

450 aromatic ring and substitution of the OH group into the ring. However, the exact position of
451 OH bond formation was not predicted and hence was shown with Markush bonds. TP2-186
452 would be formed from TP1-188 after de-hydroxylation causing loss of water, thus, creating a
453 double bond in the cyclohexane ring. TP2-186 could be present as an isomeric structure and
454 formed by either an OH radical attack on the N-alkyl group (single electron transfer) or the
455 OH radical-initiated exclusion of hydrogen atoms from carbon adjacent to the carboxylic
456 group. Another isomeric structure (TP5-187) was suggested to be formed by two different
457 pathways-

458   *i.* The OH radicals attack the amino group, dissociating the amino group (de-
459   ammonification) and oxidizing the C-terminal.
460 *ii.* Another assumption suggested the formation of the carboxylic group at the terminal
461   position after de-ammonification.

462 The gabapentin-producing high polar compounds would have caused de-hydroxylation and
463 H-atom transfer from the amino group and forming a new amino-epoxy aromatic ring (TP3-
464 154) or, the TP1-188 would have lost an amino group in combination with de-hydroxylation
465 and electron transfer to create another new epoxy aromatic structure (TP4-137). A Few of the
466 by-products formed could have rearranged the compounds after oxidation and electron
467 transfer producing closed ring structures (TP3-154, TP4-137). Certainly, hydroxylation and
468 de-ammonification appeared as the instantaneous route for gabapentin degradation
469 whereas, de-hydroxylation of gabapentin and its products formed stable aromatic
470 compounds. Overall, new carboxylic and epoxy compounds were suggested to be formed
471 after gabapentin oxidation in the Fenton process. As shown in Figure 5 (c), diuron
472 demonstrated two pathways during the Fenton process that is either an OH radical attack on
473 the alkyl group called alkyl substitution or else through chlorine substitution. Amongst both,
474 the alkyl side attack appeared to be the most spontaneous route. These routes were also
475 reported by R.R. Solís et al. during the diuron ozonation process [23]. The oxidative mechanism
476 causing each by-product formation is listed below:

477   *i.* TP1-249- Oxidative degradation- hydroxylation
478   *ii.* TP2-219- N- demethylation (Sequential electron transfer)
479 *iii.* TP3-215- Reductive chlorination and oxidative hydroxyl degradation
480   *iv.* TP4-262- Oxidative degradation- hydroxylation
481   *v.* TP5-244- Carbonyl addition, oxidation
482   *vi.* TP6-216- Reductive N-demethylation
483 *vii.* TP7-201- N-dealkylation and oxidative hydroxyl degradation

484 TP1-249 was predicted to form after hydroxylation of the C-H bond on the carbon atom
485 adjacent to the heteroatom, H-atom transfer. Subsequently, the compound was further
486 oxidized by single electron transfer from itself forming TP2-219 after N-demethylation. Few
487 of the TPs formed were suggested to be produced in a stepwise fashion while some of them
488 might have formed by direct oxidation of diuron. The chlorine substitution compounds were

489 formed separately (TP3-215). TP3-215 might exist in the isomer or either of the states. The
490 side chlorine group on the diuron has an equal affinity to withdraw an electron from the ring.
491 Therefore, the exact hydroxyl attack location was difficult to suggest, and therefore, the
492 products are presented as isomers. Likewise, the OH radical attack on the aromatic ring
493 causes an instant substitution of Cl with OH was also stated by Solís et al., 2016 [23]. TP4-262
494 was assumed to have formed after a similar mechanism of TP1-249 however; here, the C-H
495 bond was attacked from two sides on the carbon atom, binding two hydroxyl groups. The new
496 compound (TP4-262) appeared unstable, which could be possible from steric hindrance or
497 repulsion from OH groups. The electron transfer from the H-atom would have led to the H-
498 atom leaving the compound, forming an π-bond to stabilize CO after an electron transfer to
499 the second OH group. The TP6-216 was formed after sequential oxidation of diuron where
500 dealkylation conjugated with N loss followed hydroxyl attack. The new bond formed was
501 supposed to rearrange itself, forming an oxidized amino ring structure.

502 The terbutryn degradation pathway shown in Figure 5(d), suggests the triazine ring did not
503 encounter OH radical attack and remains unchanged. We confirmed it after analysis of its
504 fragment pattern which was also previously observed by Luft et al.,[24]. The Sulphur group in
505 terbutryn is a prominent nucleophilic center of the compounds which was assumed to form
506 the sulfonyl of sulfoxides compounds. TP1-240 was proposed to form by sulfur electron-

507 donating tendency which generated methylidyne-λ4-sulfanyl compound. The TP2-258 was
508 also an expected product which demonstrated sulfur oxidation and forming terbutryn-sulfur-
509 oxide. The N-ethyl terminal transferred a pair of electrons which eliminated ethane and
510 depicted a formation of lower molecular weight compound TP3-214. The TP3-214 could
511 further dissociate either to N-dealkylation or N-dealkylation accompanied by ring oxidation
512 (S-removal) and form TP4- 158, and TP6-168 respectively. TP5-256 could have been directly
513 formed from terbutryn. The methyl-thiol terminal can potentially undergo oxidation to form
514 another compound. The TP6-168 formation could involve an electron transfer from the
515 compound itself and H-atom exclusion forming a carbonyl group. The possible mechanism
516 of each by-product can be listed as:

517   *i.*   TP1-240: Methyl thiol oxidation
518   *ii.*   TP2- 258: Thiol oxidation
519   *iii.*   TP3-214: N-de-ethylation
520   *iv.*   TP4-158 : N-de-ethylation, N-2'propylation
521   *v.*   TP5-256: Methyl oxidation
522   *vi.*   TP6-168: N-dealkylation, S-de-methylation.

523 The terbuthylazine was oxidized either after an OH radical attack on the alkyl group initiating
524 alkyl removal or, the OH radical binding to the compound forming hydroxylated products
525 (Figure 4 e). The specific mechanism that could have produced the TPs was: TP1-174: N-de-
526 2'prolpylation after the cleavage of the terminal carbon-nitrogen bond in the propyl group.
527 The TP2-202 formed either by N-de-ethylation or de-hydroxylation involves the removal of

the ethyl group from the ethyl group in terbuthylazine or hydroxyl attack to the carbonyl group to TP4-244 followed by the de-hydroxylation. The N-demethylation of TP1-174 and TP2-202 could result in the formation of TP3-146. An introduction of a hydroxyl group (hydroxylation) and later oxidation of the compound to form a carbonyl group (C=O) into the molecule could form the TP4-244 (hydroxylation and carbonyl formation). A combination of two steps of substitution of chlorine with hydroxyl group (OH) through hydroxylation and removal of an ethyl group from a nitrogen atom (N-de-ethylation) would have resulted in the formation of TP5-184.

Ecological Structure Activity Relationship (ECOSAR) evaluation of Fe (0): Fenton oxidized micropollutants transformed product to predict its environmental toxicity levels

In our previous study, we used the Microtox assay to demonstrate the effective removal of toxicity associated with individual micropollutants following treatment with Fe (0) Fenton at pH 3 [6]. To further investigate the potential formation of toxic transformation products, this study aims to predict the toxicity levels of oxidized byproducts generated under Fe (0) Fenton conditions at an initial pH of 5. The toxicity to aquatic organisms – fish, daphnids, and green algae was predicted using the Ecological Structure Activity Relationship (ECOSAR) developed by the United States Environmental Protection Agency (EPA) given in Table 4 and Supplemental S7. The lower values of TPs compared to its parent compound indicate the formation of higher toxic TPs in the given micropollutant Fenton oxidation reaction. The potential TPs which could be more toxic to aquatic species compared to their parent compounds were Sulfamethoxazole TPs – TP3-284, TP4-288; Gabapentin TPs – TP3-154, TP4-137 and structural isomers of TP5-187; Diuron TP – TP1-249 and Terbutryn TPs – TP1-240, TP2-258, TP3-214. In contrast, the toxicity levels of terbuthylazine TPs were lowered to its parent compound. However, the concentration of sulfamethoxazole TPs detected was in ngL^{-1} (three magnitudes lower than the threshold values) and likewise, higher amounts of initial micropollutants were used to detect measurable TPs peaks in LC-MS, we conclude that the Fe(0) Fenton reaction catalyzed by iron powder efficiently degrade micropollutants consists of antimicrobial activity and produce low-risk oxidized products which were suggested to have reduced hazard to aquatic organisms.

Table 4 Predicted toxicity for fish, daphnid, and green algae of sulfamethoxazole, gabapentin, diuron, terbutryn, terbuthylazine, and their transformed products (TPs) measured as acute and chronic values.

Compound	Fish 96h LC$_{50}$	Daphnid 48h LC$_{50}$	Green Algae 96h EC$_{50}$	Fish Chro V	Daphnid Chro V	Green Algae Chro V
Sulfamethoxazole (SMx)	4780	2360	986	396	156	189
SMx-TP1	13700	6480	2250	548	na	na
SMx-TP2	96200	41700	11000	6830	1910	1450

Compound	Fish [96h] LC$_{50}$	Daphnid[4] [8h] LC$_{50}$	Green Algae[96h] EC$_{50}$	Fish Chro V	Daphnid Chro V	Green Algae Chro V
SMx-TP3	*920*	*491*	*284*	*83.70*	*40.40*	*65*
SMx-TP4	*4590*	*21.30*	*98.60*	*181*	*0.19*	*107*
SMx-TP5	6950	3230	1060	537	181	178
Gabapentin (GBp)	53900	4340	7770	10400	243	1940
GBp-TP1	na	na	na	na	na	na
GBp-TP2i	319X10^4	1160 X10^4	138 X10^4	185 X10^4	329000	134000
GBp-TP2ii	6070 X10^4	2150 X10^4	226 X10^4	340 X10^4	562000	207000
GBp-TP3	*150*	*84.60*	*61*	*14.50*	*8.07*	*15.70*
GBp-TP4	*24.30*	*14.80*	*14.60*	*2.57*	*1.74*	*4.44*
GBp-TP5i	28600	14200	6180	2390	965	1210
GBp-TP5ii	*4500*	*2440*	*1490*	*416*	*208*	*350*
Diuron (Diu)	47.70	28.80	27.70	5.01	3.34	8.34
Diu-TP1	*23.30*	*14.50*	*16.00*	*2.55*	*1.84*	*5.17*
Diu-TP2	69.30	41.10	36.50	7.12	4.51	10.50
Diu-TP3i	928	489	268	83.10	38.80	59.60
Diu-TP3ii	928	489	268	83.10	38.80	59.60
Diu-TP4	1810	935	471	158	70.10	100
Diu-TP5	377	208	138	35.70	18.80	34.10
Diu-TP6	89.80	52.60	44.50	9.10	5.59	12.50
Diu-TP7	103	59.90	48.80	10.30	6.20	13.40
Terbutryn (TBr)	5.11	3.42	5.00	0.61	0.53	1.88
TBr-TP1	*4.40*	*2.80*	*4.25*	*0.50*	*0.44*	*1.63*
TBr-TP2	*2.67*	*1.84*	*3.08*	*0.33*	*0.31*	*1.25*
TBr-TP3	*7.68*	*1.44*	*3.30*	*0.06*	*0.02*	*0.67*
TBr-TP4	1480	753	358	127	54.30	73.50
TBr-TP5	34	20.90	21.80	3.66	2.56	6.85
TBr-TP6	322	176	112	30.10	15.40	27
Terbuthylazine (TBz)	**13.60**	**8.70**	**10.50**	**1.53**	**1.18**	**3.58**
TBz-TP1	534	286	167	48.70	23.70	38.30
TBz-TP2	102	59.40	48.40	10.30	6.15	13.30
TBz-TP3	3830	1860	732	312	118	136
TBz-TP4	135	78.10	62.60	13.50	8	17
TBz-TP5	417	226	140	38.70	19.40	33.10

LC$_{50}$: Half lethal concentration, **EC$_{50}$:** Half effective concentration, both representing the acute toxicity; **Chro V:** Chronic Value representing chronic toxicity. Chro V was measured as a geometric mean of the number of observed effect concentrations and the lowest observed effect concentrations. The above values are for neutral organic compounds measured in **mgL^{-1}**. The compound **bold** and in *italics* indicate that the given transformed product (TP) has high toxicity compared to its parent compound.

Discussion

561

562 Fenton Oxidation is a promising technology for the removal of emerging micropollutants
563 from water, involving the generation of non-selective hydroxyl radicle (•OH) from H_2O_2
564 disintegration catalyzed by Fe^{2+} species [31][32]. Despite its non-selective oxidation mechanism,
565 Fenton oxidation is not yet widely used at the industrial scale due to some of the critical
566 challenges such as excessive sludge production and requirements of high acidic
567 environment. However, several studies have intervened in these challenges and have used
568 Fenton in combination with other technologies [33][34][35][36]. Studies have also reformed the
569 catalyst to transform the reaction to a heterogeneous Fenton Oxidation [7][37][38]. We have used
570 iron powder as a Fe (0) catalyst in the Fenton reaction and established the modified Fenton
571 Oxidation Process which synergistically oxidizes and adsorbs micropollutants thereby
572 increasing the effectiveness of the treatment. In our previous research, we have
573 demonstrated that using Fe (0) significantly reduces sludge production and increases the
574 removal of dissolved organic (DOC) at pH 3 [6][7]. Herein, in this study, we found that the Fe (0)
575 Fenton Oxidation treatment could achieve about 70-to-100% degradation of organic
576 compounds at pH 5 (Figure 1). The difference in the degradation efficiency was suggested to
577 be influenced by the target compound structure and properties. In addition to estimating the
578 treatment efficiency, TPs could also be used to study the mechanistic approach of the
579 Fenton reaction understanding its specificity and susceptible or resistant compounds to
580 Fenton reactions. Most of the oxidation TPs identified in this study were also found in
581 Ozonation and other oxidation treatment [22][20, 23, 27, 28][27] suggesting the commonality in the
582 oxidation mechanism of •OH capable of oxidizing target compound. The type of reaction
583 between the target compound and the •OH, largely influences the rate and extent of
584 degradation.

585 Hydrogen abstraction, addition, and electron transfer were the most common modes of
586 action observed in our study. In addition to the removal or addition of the OH group, de-
587 alkylation, and hydrogenation were the most common mechanisms observed in the
588 formation of TPs where the target compounds were degraded to low molecular weight
589 compounds. Overall, the suites of oxidative mechanism and modification in functional
590 groups observed in this study include ***i)*** hydroxylation, ***ii)*** de-hydroxylation, ***iii)***
591 hydrogenation, ***iv)*** N-dealkylation, ***v)*** methyl oxidation, ***vi)*** thiol oxidation or reduction, **vii)**
592 amino-group oxidation, **vii)** C-oxidation (R—CO, R—COOH), **ix)** Cl group substitution and **x)**
593 alkyl group substitution. Steric hindrance due to the presence of an alkyl group in the
594 compound was also suggested as an influencing factor in Fenton Oxidation. Particularly,
595 terbutryn and terbuthylazine differ in the sixth position, which might be the primary cause
596 for the vast difference in their stability. The methyl sulfonyl group (Thiol) in Terbutryn was
597 found to be more susceptible to oxidation reactions. The thiol oxidation was facilitated with
598 OH and thus able to destabilize the triazine structure. Consequently, terbutryn was more
599 easily degraded than terbuthylazine.

The heteroatoms like Cl and S were substituted and oxidized however, the presence of Cl was also found as a resistance to Fenton reaction in some of the diuron TPs. Cl atom is electronegative and has an electron-withdrawing nature which could have resulted in compromising the effective degradation of diuron and its TPs. Except for TP3-215 where either of the terminal Cl was substituted with OH, the rest of the TP's has retained its aromaticity and chloro-substituents. The N-alkyl and amide groups were the primed mode of oxidation observed in diuron degradation. Similarly, the amine and carboxylic acid functional groups present in gabapentin were identified as primary target sites for hydroxyl radical attack during the Fenton oxidation. Overall, we observed that the aromatic ring was stable, and aliphatic compounds and functional groups were more readily attacked and transformed during the Fe (0) Fenton oxidation reactions.

Assessing the toxicity of transformation products (TPs) generated during water treatment is crucial for evaluating potential environmental and human health risks. In this study, sulfamethoxazole TPs were detected at low ng/L concentrations in the effluent, suggesting the occurrence of ring-opening and subsequent mineralization. While the low ng/L concentrations of sulfamethoxazole TPs are encouraging, further investigations would be required for the potential long-term impacts. The environmental fate of the TPs identified is critical to understand its persistence and impact on the ecosystem. A few of the oxidized products detected in this study were also identified by other authors in aquatic ecosystems. The sulfamethoxazole TPs—TP3-284, TP6-254, and TP5-99 were the biodegradative products detected by Su et al., 2016 [30].

Gabapentin is not metabolized by the human body and is excreted in its intact form. Thereby, the biodegradation of gabapentin occurring in the environment would determine its environmental fate. Gabapentin TPs — TP1-188, TP3-154, and TP5-187 were also detected by Henning et al., 2018 as bio-transformed products of gabapentin in the aquatic environments [39]. Diuron, a phenyl urea herbicide, has been widely used in agricultural and non-agricultural settings to control weed growth. However, its persistence in the environment and toxicity to aquatic organisms have raised significant concerns[40]. In response to growing scientific evidence, the U.S. Environmental Protection Agency (EPA) proposed a ban on diuron use in all food crop production in April 2022[41]. This regulatory action was primarily driven by concerns over diuron's potential carcinogenic properties. The metabolic pathway of bacterial degradation of diuron in aerobic conditions includes TP2-219 as an intermediate compound to form 3,4-dichloroaniline [40, 42].

A study by Bollmann et al. 2016 [43] also detected TP2-258 and TP6-168 terbutryn products where these products were studied as a leached compound from artificial walls under natural weather conditions after the photodegradation process. Similar to terbutryn, terbuthylazine is a triazine-class pesticide widely used as an alternative to atrazine in agricultural fields. However, the environmental fate is yet to be fully understood. We identified five oxidized transformed products that were predicted to have low risk to the

aquatic species. Recently, bacteria such as *Agrobacterium* and others have been found to degrade terbuthylazine, the TP5-184, detected in this study was also identified as the catabolism pathway of bacterial degradation of terbuthylazine. Thereby, the simultaneous shared compounds between the oxidation TPs and microbial degradation of a target micropollutant could be further investigated to study the complex interplay between these compounds and their fate in the environment.

Conclusion

The Fenton oxidation process is a developing technology that holds the potential to effectively remove antimicrobials and other emerging contaminants in water. We have developed a novel use of commercially available iron powder (Fe (0)) as a catalyst in the Fenton reaction as a promising alternative to existing homogeneous Fenton. We selected five important emerging contaminants in our study which were also observed to pertain to carcinogenic and antimicrobial activities and thus harmful to human health and the environment. At initial pH 5, the iron powder catalyzed Fenton reaction achieved complete oxidation of sulfamethoxazole and terbutryn, 90 to 100% removal of Diuron, 80 to 90% Gabapentin removal, and about 65 to 70% removal of terbuthylazine. The tandem mass spectrometry detected and confirmed the transformation products formed during the treatment. The sulfamethoxazole and its transformed products were detected at trace levels after 40 min and thus suggested as the best optimal reaction time for sulfamethoxazole removal. These results expand the area of experiment design and optimization and suggest that studying the formation of transformed products can lead to an informed and high-yield treatment optimization. The identification of transformation products formed provided a critical insight into the Fe (0)-Fenton Oxidation mechanisms and hence the degradation pathway was suggested.

Acknowledgments

Figures

Figure 1 Degradation of selected micropollutants in zero-valent iron (Fe (0)) catalyzed Fenton Oxidation process. The initial solution of each micropollutant prepared in distilled Milli Q water was adjusted to pH 5 before treatment. Fenton reaction was initiated immediately after adding optimal H_2O_2 to the test solution. The optimal reaction time and molar ratio of H_2O_2: Fe (0) was used to quantify the degradation efficiency of treatment at pH 5.
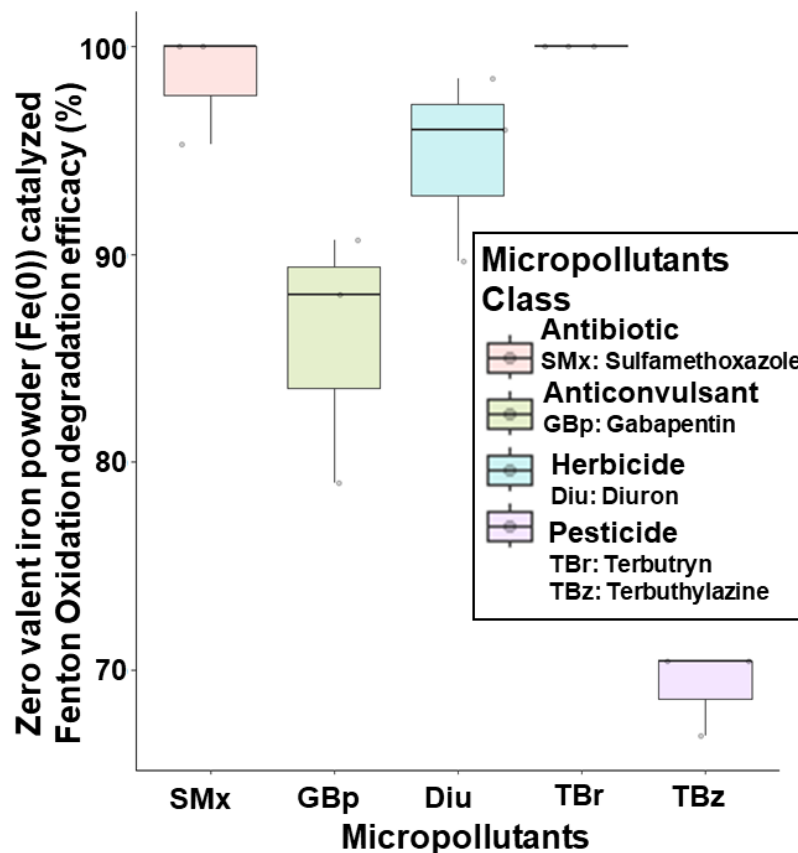
Figure 2. LC-MS spectra of transformed product after zero valent iron powder Fe (0) Fenton Oxidation **a.** ESI (+) of sulfamethoxazole; gabapentin **b.** ESI (+); **c.** ESI (-); diuron **d.** ESI (+); **e.** ESI (-); **f.** ESI (+) terbutryn; **g.** ESI (+) terbuthylazine. Comprehensive LC-MS spectra of each micropollutant oxidized transformed product are given in Supplementary Figure 1.
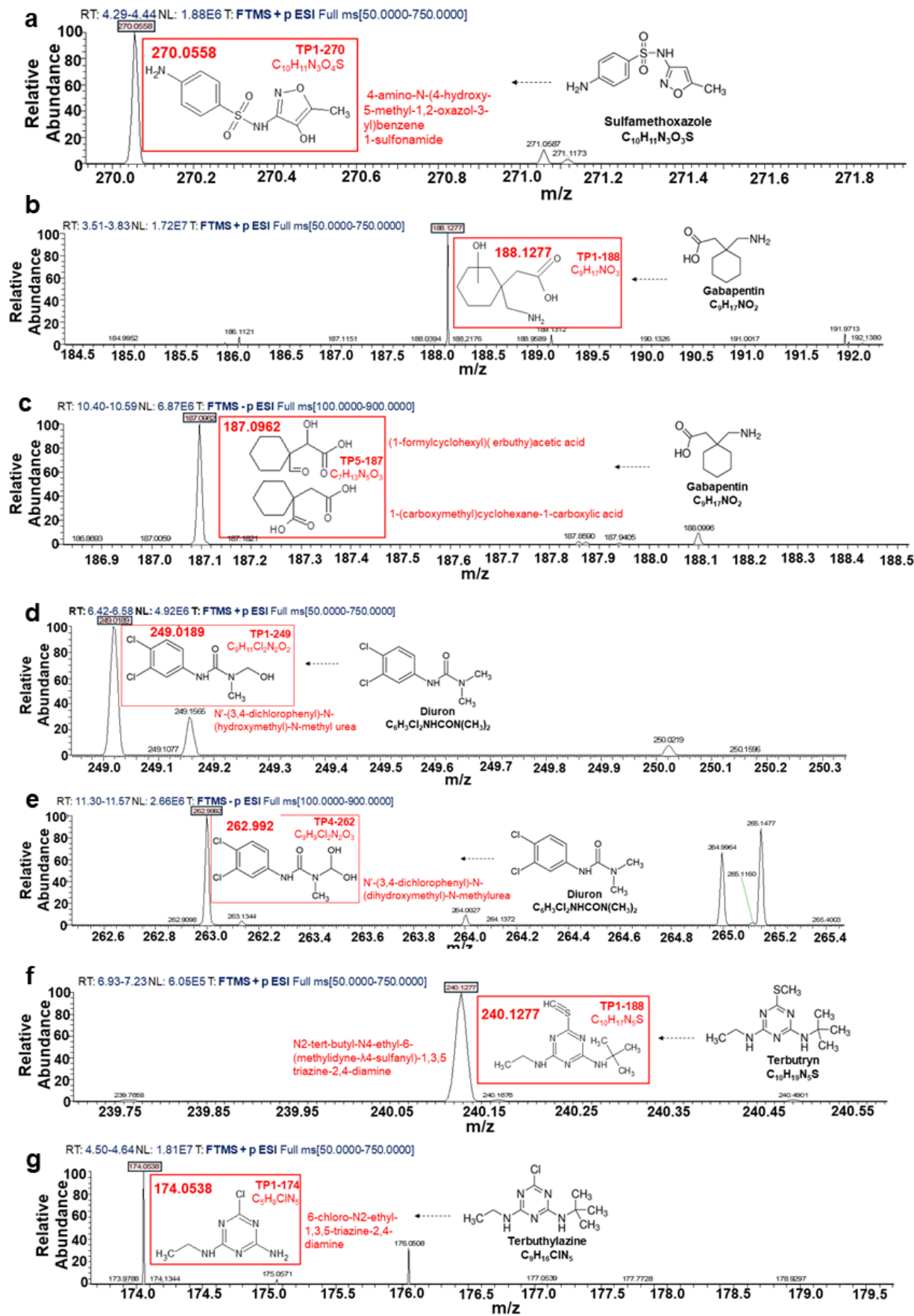
Figure 3. Relative abundance of transformed products TP isotopes (represented by different m/z values). The left section in dotted boundaries has data points that demonstrate the relative abundance of isotopes of prevalent TPs'. The right boundary has the molecular formula of prevalent TPs numbered from 1 to 29. The color of the data points is assigned to its parent compound. The relative abundance is the measure of the abundance of TP's accurate m/z. The relative abundance of TP from 26 to 28 on the right box was < 95%.
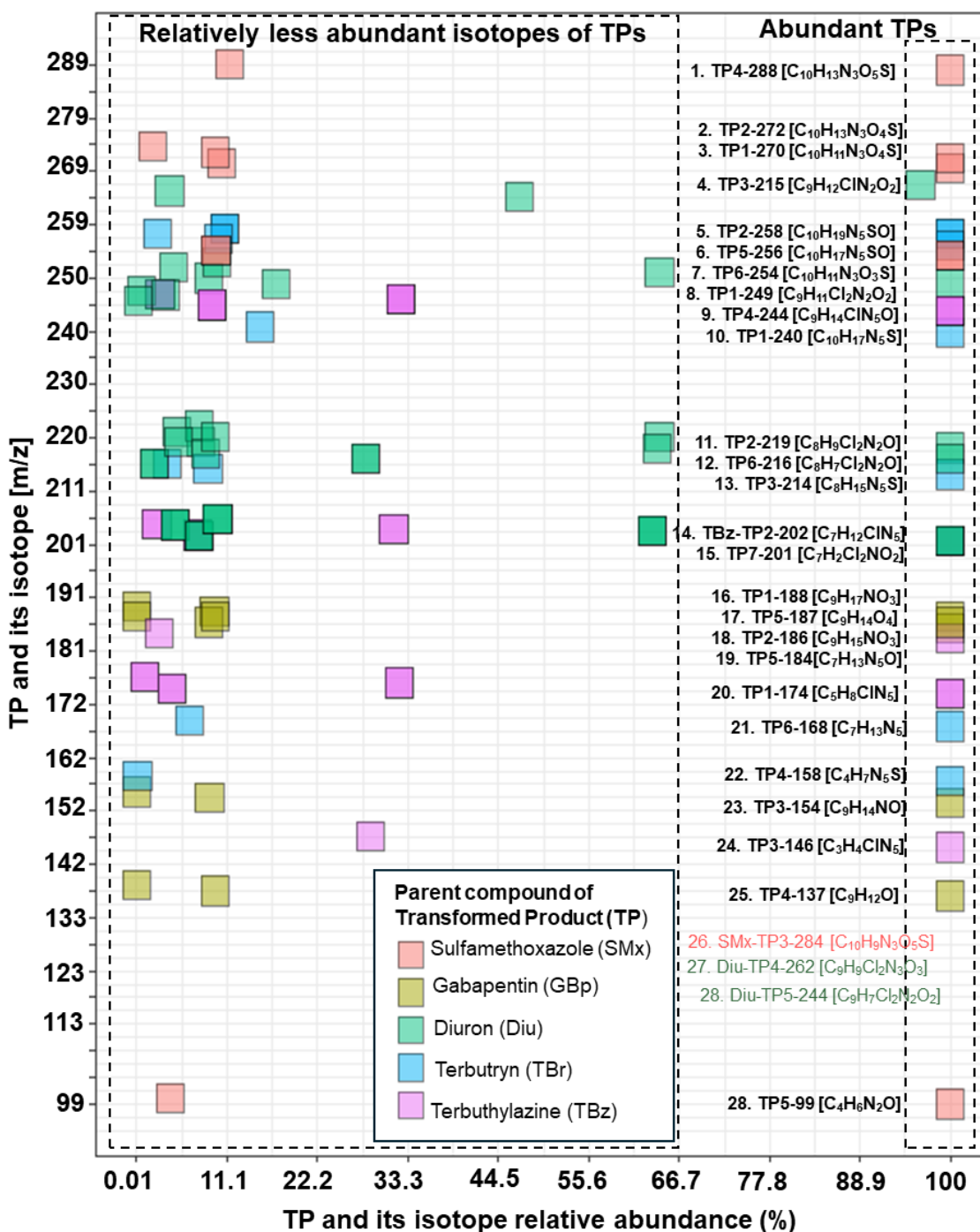
Figure 4. (a-d) Fragment pattern identifying the product ion of sulfamethoxazole oxidized transformed products **(a)** TP1-270: *4-amino-N-(4-hydroxy-5-methyl-1,2-oxazol-3-yl)benzene-1-sulfonamide*, **(b)** TP5-99: *5-methyl-1,2-oxazol-3-amine*, **(c)** TP2-272: *4-amino-N-(4-hydroxy-5-methyl-4,5-dihydro-1,2-oxazol-3-yl)benzene-1-sulfonamide*, **(d)** TP4-288: *4-amino-N-(4,5-dihydroxy-5-methyl-4,5-dihydro-1,2-oxazol-3-yl)benzene-1-sulfonamide*; **(e)** Rate of change (Δ) in sulfamethoxazole and formation or disappearance of its transformed products as a function of time during the Fe(0)- Fenton Process. Δ was estimated as a ratio of the difference in m/z intensity of ions at a given time (t) from its initial intensity and the difference in treatment time (t- 1).
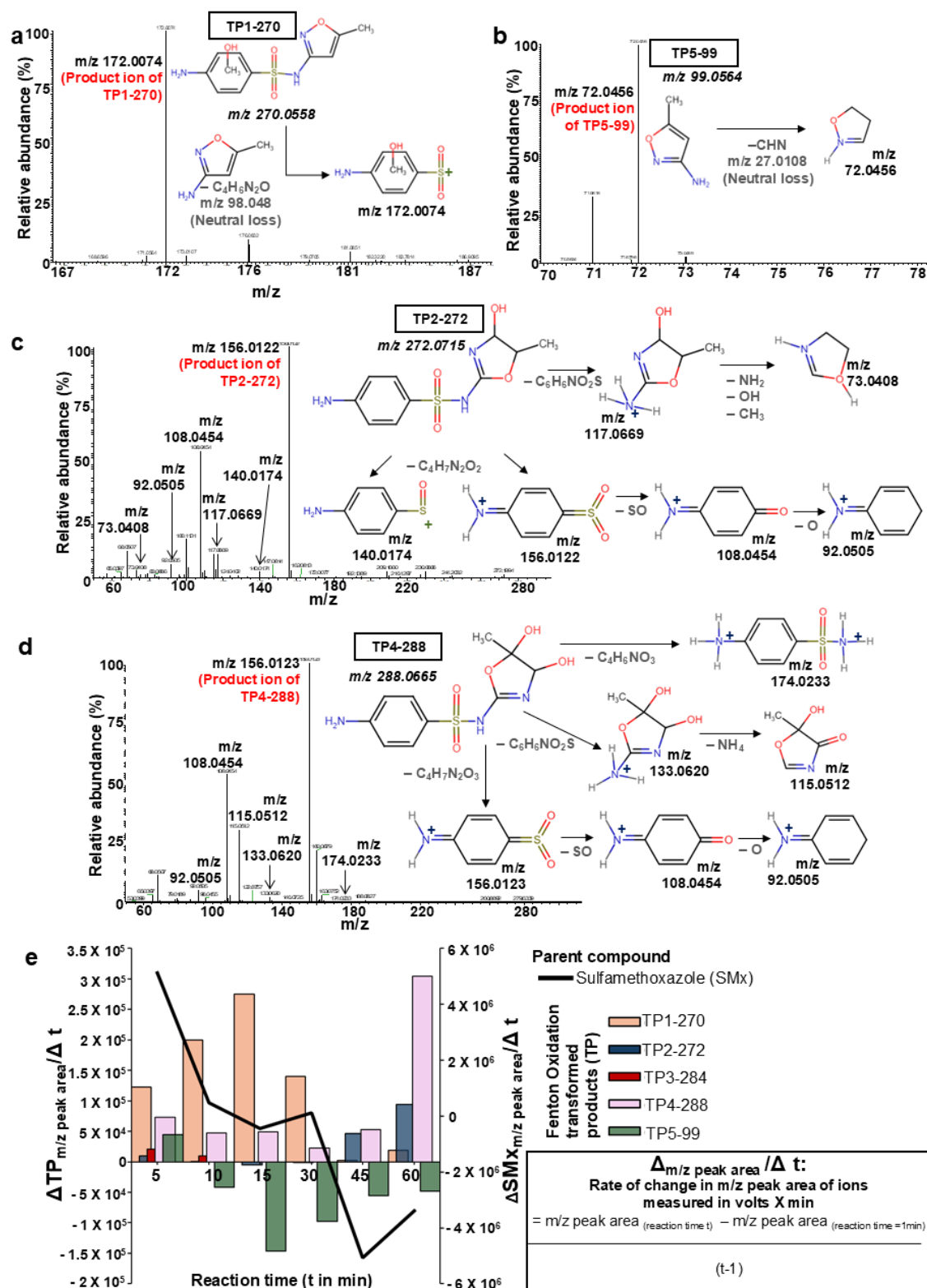
Figure 5. Oxidation transformation reaction scheme of studied micropollutants in zero-valent iron Fe (0) – Fenton Oxidation process at pH 5 **(a)** Sulfamethoxazole, **(b)** Gabapentin, **(c)** Diuron, **(d)** Terbutryn and **(e)** Terbuthylazine.
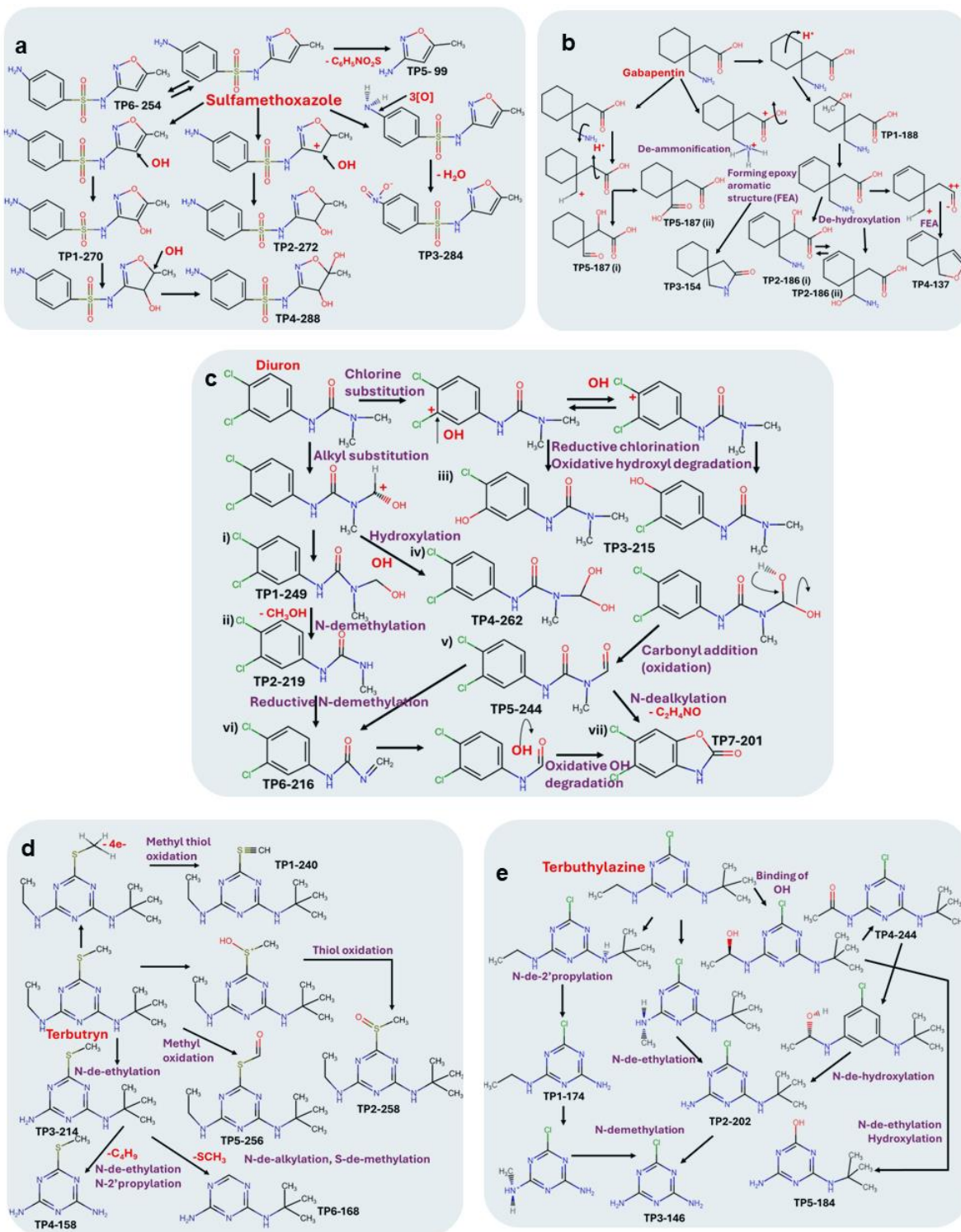
References

(1) Kusi, J.; Ojewole, C. O.; Ojewole, A. E.; Nwi-Mozu, I. Antimicrobial Resistance Development Pathways in Surface Waters and Public Health Implications. *Antibiotics (Basel)* **2022**, *11* (6). DOI: 10.3390/antibiotics11060821 From NLM PubMed-not-MEDLINE.

(2) Grenni, P. Antimicrobial Resistance in Rivers: A Review of the Genes Detected and New Challenges. *Environ Toxicol Chem* **2022**, *41* (3), 687-714. DOI: 10.1002/etc.5289 From NLM Medline.

(3) Singh, A. K.; Kaur, R.; Verma, S.; Singh, S. Antimicrobials and Antibiotic Resistance Genes in Water Bodies: Pollution, Risk, and Control. *Frontiers in Environmental Science* **2022**, *10*. DOI: 10.3389/fenvs.2022.830861.

(4) Organization, W. H. *Ten threats to global health in 2019*. 2019. https://www.who.int/news-room/spotlight/ten-threats-to-global-health-in-2019 (accessed 2024 May 9).

(5) Ramírez-Melgarejo, M.; Stringer, T. Wastewater treatment, energy consumption, and greenhouse gas emissions: An operational approach to comparing Barcelona and Mexico City. *Journal of Environmental Management* **2024**, *353*, 120175. DOI: https://doi.org/10.1016/j.jenvman.2024.120175. Maktabifard, M.; Al-Hazmi, H. E.; Szulc, P.; Mousavizadegan, M.; Xu, X.; Zaborowska, E.; Li, X.; Mąkinia, J. Net-zero carbon condition in wastewater treatment plants: A systematic review of mitigation strategies and challenges. *Renewable and Sustainable Energy Reviews* **2023**, *185*, 113638. DOI: https://doi.org/10.1016/j.rser.2023.113638.

(6) Goswami, A.; Jiang, J.-Q.; Petri, M. Treatability of five micro-pollutants using modified Fenton reaction catalysed by zero-valent iron powder (Fe(0)). *Journal of Environmental Chemical Engineering* **2021**, *9* (4), 105393. DOI: https://doi.org/10.1016/j.jece.2021.105393.

(7) Goswami, A.; Jiang, J.-Q. Comparative Performance of Catalytic Fenton Oxidation with Zero-Valent Iron (Fe(0)) in Comparison with Ferrous Sulphate for the Removal of Micropollutants. *Applied Sciences* **2019**, *9* (11). DOI: 10.3390/app9112181.

(8) Trellu, C.; Oturan, N.; Keita, F. K.; Fourdrin, C.; Pechaud, Y.; Oturan, M. A. Regeneration of Activated Carbon Fiber by the Electro-Fenton Process. *Environ Sci Technol* **2018**, *52* (13), 7450-7457. DOI: 10.1021/acs.est.8b01554.

(9) Forooshani, P. K.; Pinnaratip, R.; Polega, E.; Tyo, A. G.; Pearson, E.; Liu, B.; Folayan, T. O.; Pan, L.; Rajachar, R. M.; Heldt, C. L.; et al. Hydroxyl Radical Generation Through the Fenton-Like Reaction of Hematin- and Catechol-Functionalized Microgels. *Chem Mater* **2020**, *32* (19), 8182-8194. DOI: 10.1021/acs.chemmater.0c01551. Grossman, J. N.; Kahan, T. F. Hydroxyl radical formation from bacteria-assisted Fenton chemistry at neutral pH under environmentally relevant conditions. *Environmental Chemistry* **2016**, *13* (4), 757-766. DOI: https://doi.org/10.1071/EN15256. Barbusiński, K. Fenton reaction - controversy concerning the chemistry. *Ecological Chemistry and Engineering S-chemia I Inzynieria Ekologiczna S* **2009**, *16*, 347-358.

(10) Lynch, M.; Kuramitsu, H. Expression and role of superoxide dismutases (SOD) in pathogenic bacteria11Address for correspondence: Division of Science, American Dental Association, 211 E. Chicago Ave., Chicago, IL 60611, USAFormerly aDepartments of Oral Biology and bPeriodontology, State University of New York, Buffalo, New York 14214, USA, and cVeterans Administration Medical Center, Buffalo, New York, USA. *Microbes and Infection* **2000**, *2* (10), 1245-1255. DOI: https://doi.org/10.1016/S1286-4579(00)01278-8. Wang, Y.; Branicky, R.; Noe, A.; Hekimi, S. Superoxide dismutases: Dual roles in controlling ROS damage and regulating ROS signaling. *J Cell Biol* **2018**, *217* (6), 1915-1928. DOI: 10.1083/jcb.201708007.

(11) Fernández-Calviño, D.; Rousk, J.; Bååth, E.; Bollmann, U. E.; Bester, K.; Brandt, K. K. Short-term toxicity assessment of a triazine herbicide (terbutryn) underestimates the sensitivity of soil

microorganisms. *Soil Biology and Biochemistry* **2021**, *154*, 108130. DOI: https://doi.org/10.1016/j.soilbio.2021.108130. Baćmaga, M.; Wyszkowska, J.; Borowik, A.; Kucharski, J. Effect of sulcotrione and terbuthylazine on biological characteristics of soil. *Applied Soil Ecology* **2024**, *195*, 105232. DOI: https://doi.org/10.1016/j.apsoil.2023.105232. Thomas, M. C.; Flores, F.; Kaserzon, S.; Reeks, T. A.; Negri, A. P. Toxicity of the herbicides diuron, propazine, tebuthiuron, and haloxyfop to the diatom Chaetoceros muelleri. *Scientific Reports* **2020**, *10* (1), 19592. DOI: 10.1038/s41598-020-76363-0. Kruszewska, H.; Zaręba, T.; Tyski, S. Examination of antimicrobial activity of selected non-antibiotic products. *Acta poloniae pharmaceutica* **2010**, *67* 6, 733-736. Eliopoulos, G. M.; Huovinen, P. Resistance to Trimethoprim-Sulfamethoxazole. *Clinical Infectious Diseases* **2001**, *32* (11), 1608-1614. DOI: 10.1086/320532 (acccessed 7/18/2024).

(12) DRUGBANKOnline. *Sulfamethoxazole*. 2005. https://go.drugbank.com/drugs/DB01015 (accessed 2024 August 20).

(13) DRUGBANKOnline. *Gabapentin*. 2005. https://go.drugbank.com/drugs/DB00996 (accessed 2024 August 20).

(14) Drugs.com. *Gabapentin*. https://www.drugs.com/gabapentin.html (accessed.

(15) Brewer, K.; Machin, J.; Maylin, G.; Fenger, C.; Morales-Briceño, A.; Tobin, T. Gabapentin, a human therapeutic medication and an environmental substance transferring at trace levels to horses: a case report. *Irish Veterinary Journal* **2022**, *75* (1), 19. DOI: 10.1186/s13620-022-00226-5. Ferencik, M.; Blahova, J.; Schovankova, J.; Siroka, Z.; Svobodova, Z.; Kodes, V.; Stepankova, K.; Lakdawala, P. Residues of Selected Anticonvulsive Drugs in Surface Waters of the Elbe River Basin (Czech Republic). *Water* **2022**, *14* (24). DOI: 10.3390/w14244122.

(16) Jabbour, M.; Al-Khayat, M. A.; Al-Ktaifani, M.; Yernale, N. G. Synthesis, Characterization, and Biological Evaluation of Gabapentinoid Hybrids with Isoindole-1,3(2H)-Dione Moiety as Potential Antioxidant, Antimicrobial, and Anticancer Agents. *Journal of Chemistry* **2023**, *2023*, 1-16. DOI: 10.1155/2023/8992853.

(17) Michelle L. Hladik , D. L. C. *Analysis of the herbicide diuron, three diuron degradates, and six neonicotinoid insecticides in water—Method details and application to two Georgia streams: U.S. Geological Survey Scientific Investigations Report 2012–5206*; U.S. Geological Survey, Virginia, 2012. DOI: http://pubs.usgs.gov/sir/2012/5206.

(18) Liu, J. Diuron. In *Encyclopedia of Toxicology (Third Edition)*, Wexler, P. Ed.; Academic Press, 2014; pp 215-216.

(19) Christine Hartless, M. J., Fred Jenkins, James Lin, Anita Ullagaddi. *Risks of 2,4-D Use to the Federally Threatened California Red-legged Frog (Rana aurora draytonii) and Alameda Whipsnake (Masticophis lateralis euryxanthus)*; Environmental Fate and Effects Division Office of Pesticide Programs Washington, D.C. 20460, 2009. https://www3.epa.gov/pesticides/endanger/litstatus/effects/redleg-frog/2-4-d/analysis.pdf.

(20) Ormad, M. P.; Miguel, N.; Lanao, M.; Mosteo, R.; Ovelleiro, J. L. Effect of Application of Ozone and Ozone Combined with Hydrogen Peroxide and Titanium Dioxide in the Removal of Pesticides From Water. *Ozone: Science & Engineering* **2010**, *32* (1), 25-32. DOI: 10.1080/01919510903482764.

(21) Álvarez, P. M.; Quiñones, D. H.; Terrones, I.; Rey, A.; Beltrán, F. J. Insights into the removal of terbuthylazine from aqueous solution by several treatment methods. *Water Research* **2016**, *98*, 334-343. DOI: https://doi.org/10.1016/j.watres.2016.04.026.

(22) Yang, Y.; Lu, X.; Jiang, J.; Ma, J.; Liu, G.; Cao, Y.; Liu, W.; Li, J.; Pang, S.; Kong, X.; et al. Degradation of sulfamethoxazole by UV, UV/H2O2 and UV/persulfate (PDS): Formation of oxidation products and effect of bicarbonate. *Water Research* **2017**, *118*, 196-207. DOI: https://doi.org/10.1016/j.watres.2017.03.054.

(23) Solís, R. R.; Rivas, F. J.; Martínez-Piernas, A.; Agüera, A. Ozonation, photocatalysis and photocatalytic ozonation of diuron. Intermediates identification. *Chemical Engineering Journal* **2016**, *292*, 72-81. DOI: https://doi.org/10.1016/j.cej.2016.02.005.

(24) Luft, A.; Wagner, M.; Ternes, T. A. Transformation of Biocides Irgarol and Terbutryn in the Biological Wastewater Treatment. *Environmental Science & Technology* **2014**, *48* (1), 244-254. DOI: 10.1021/es403531d.

(25) Patiny, L.; Borel, A. ChemCalc: A Building Block for Tomorrow's Chemical Infrastructure. *Journal of Chemical Information and Modeling* **2013**, *53* (5), 1223-1228. DOI: 10.1021/ci300563h.

(26) Rose, A. S.; Bradley, A. R.; Valasatava, Y.; Duarte, J. M.; Prlić, A.; Rose, P. W. NGL viewer: web-based molecular graphics for large complexes. *Bioinformatics* **2018**, *34* (21), 3755-3758. DOI: 10.1093/bioinformatics/bty419 (acccessed 8/20/2024).

(27) Herrmann, M.; Menz, J.; Olsson, O.; Kümmerer, K. Identification of phototransformation products of the antiepileptic drug gabapentin: Biodegradability and initial assessment of toxicity. *Water Research* **2015**, *85*, 11-21. DOI: https://doi.org/10.1016/j.watres.2015.08.004.

(28) Pereira, S. V.; Reis, T.; Souza, B. S.; Dantas, R. F.; Azevedo, D. A.; Dezotti, M.; Sans, C.; Esplugas, S. Oestrogenicity assessment of s-triazines by-products during ozonation. *Environmental Technology* **2015**, *36* (12), 1538-1546. DOI: 10.1080/09593330.2014.995235.

(29) Ouyang, W.-Y.; Birkigt, J.; Richnow, H. H.; Adrian, L. Anaerobic Transformation and Detoxification of Sulfamethoxazole by Sulfate-Reducing Enrichments and Desulfovibrio vulgaris. *Environmental Science & Technology* **2021**, *55* (1), 271-282. DOI: 10.1021/acs.est.0c03407.

(30) Su, T.; Deng, H.; Benskin, J. P.; Radke, M. Biodegradation of sulfamethoxazole photo-transformation products in a water/sediment test. *Chemosphere* **2016**, *148*, 518-525. DOI: https://doi.org/10.1016/j.chemosphere.2016.01.049.

(31) Fenton, H. J. H. Oxidation of Tartaric Acid in Presence of Iron. *Journal of the Chemical Society, Transactions* **1894**, *65*, 899-910. DOI: https://doi.org/10.1039/CT8946500899.

(32) David A. Wink, R. W. N., Joseph E. Saavedra, William E. Utermahlen, Jr.T, Peter C. Ford. The Fenton oxidation mechanism: Reactivities of biologically

relevant substrates with two oxidizing intermediates differ

from those predicted for the hydroxyl radical. *The Proceedings of the National Academy of Sciences* **1994**, *91*, 6604-6608.

(33) Walling, S. A.; Um, W.; Corkhill, C. L.; Hyatt, N. C. Fenton and Fenton-like wet oxidation for degradation and destruction of organic radioactive wastes. *npj Materials Degradation* **2021**, *5* (1), 50. DOI: 10.1038/s41529-021-00192-3.

(34) Min, X.; Changyong, W.; Yuexi, Z. Advancements in the Fenton Process for Wastewater Treatment. In *Advanced Oxidation Processes*, Ciro, B.-L. Ed.; IntechOpen, 2020; p Ch. 4.

(35) Mokhbi, Y.; Korichi, M.; Akchiche, Z. Combined photocatalytic and Fenton oxidation for oily wastewater treatment. *Applied Water Science* **2019**, *9* (2), 35. DOI: 10.1007/s13201-019-0916-x.

(36) Thomas, N.; Dionysiou, D. D.; Pillai, S. C. Heterogeneous Fenton catalysts: A review of recent advances. *Journal of Hazardous Materials* **2021**, *404*, 124082. DOI: https://doi.org/10.1016/j.jhazmat.2020.124082.

(37) Chen, Y.; Miller, C. J.; Waite, T. D. Heterogeneous Fenton Chemistry Revisited: Mechanistic Insights from Ferrihydrite-Mediated Oxidation of Formate and Oxalate. *Environmental Science & Technology* **2021**, *55* (21), 14414-14425. DOI: 10.1021/acs.est.1c00284.

(38) Pereira, M. C.; Oliveira, L. C. A.; Murad, E. Iron oxide catalysts: Fenton and Fentonlike reactions – a review. *Clay Minerals* **2012**, *47* (3), 285-302. DOI: 10.1180/claymin.2012.047.3.01 From Cambridge University Press Cambridge Core.

(39) Henning, N.; Kunkel, U.; Wick, A.; Ternes, T. A. Biotransformation of gabapentin in surface water matrices under different redox conditions and the occurrence of one major TP in the aquatic environment. *Water Res* **2018**, *137*, 290-300. DOI: 10.1016/j.watres.2018.01.027 From NLM Medline.

(40) Giacomazzi, S.; Cochet, N. Environmental impact of diuron transformation: a review. *Chemosphere* **2004**, *56* (11), 1021-1032. DOI: https://doi.org/10.1016/j.chemosphere.2004.04.061.

(41) EPA. *EPA Seeks Public Comment on Measures to Address Human Health and Ecological Risks Posed by Diuron*; 2022. https://www.epa.gov/pesticides/epa-seeks-public-comment-measures-address-human-health-and-ecological-risks-posed-diuron (accessed 8/19/2024).

(42) Sørensen, S. R.; Bending, G. D.; Jacobsen, C. S.; Walker, A.; Aamand, J. Microbial degradation of isoproturon and related phenylurea herbicides in and below agricultural fields. *FEMS Microbiology Ecology* **2003**, *45* (1), 1-11. DOI: https://doi.org/10.1016/S0168-6496(03)00127-2.

(43) Bollmann, U. E.; Minelgaite, G.; Schlüsener, M.; Ternes, T.; Vollertsen, J.; Bester, K. Leaching of Terbutryn and Its Photodegradation Products from Artificial Walls under Natural Weather Conditions. *Environmental Science & Technology* **2016**, *50* (8), 4289-4295. DOI: 10.1021/acs.est.5b05825.